Antioxidant and antibacterial lignin nanoparticles in polyvinyl alcohol/chitosan films for active packaging

W. Yang[1], J. S. Owczarek[2], E. Fortunati[1], M. Kozanecki[2], A. Mazzaglia[3], G.M. Balestra[3], J. M. Kenny[1], L. Torre[1], D. Puglia[1]*

[1]*University of Perugia, Civil and Environmental Engineering Department, Materials Engineering Center, UdR INSTM, Terni – Italy*
[2]*Lodz University of Technology, Department of Molecular Physics, Lodz - Poland*
[3]*University of Tuscia, Department of Agricultural Sciences and Forestry (DAFNE), Viterbo – Italy*

**Corresponding author: debora.puglia@unipg.it*, Tel +390744492916; Fax +390744492950

Abstract

Binary and ternary polymeric films based on polyvinyl alcohol (PVA), chitosan (CH) and lignin nanoparticles (LNP) added at two different amounts (1 and 3 wt %) were produced by solvent casting. Thermal, optical, mechanical properties, migration, antioxidant and antibacterial activities, as well as morphologies of binary and ternary PVA/CH/LNP nanocomposites, were investigated. Mechanical results revealed that the addition of LNP enhanced the tensile strength and Young's modulus of PVA, producing also a toughness effect in CH matrix. Higher cristallinity values measured in calorimetric characterization confirmed how well dispersed LNP could effectively provide nucleation effects in PVA. Furthermore, LNP notably improved the thermal stability of the binary and ternary nanocomposite systems. In addition, LNP and CH synergically influenced the antioxidation response of the produced films, on the basis of disappearance, at 517 nm, of 2,2-diphenyl-1-picrylhydrazyl (DPPH) absorption band. Overall migration tests showed that the migration level is well below the legislative limits for food contact materials, whereas antimicrobial assays revealed a capacity to inhibit the bacterial growth of Gram negative *Erwinia carotovora* subsp. *carotovora* and *Xanthomonas arboricola* pv. *pruni* over the time, suggesting innovative opportunities against bacterial plant/fruit pathogens.

Keywords: polyvinyl alcohol, chitosan, lignin nanoparticles, nanocomposites, bacterial plant pathogens, antioxidant activity.

1 Introduction

The need of using environmentally and eco-friendly materials, in substitution of other traditional non-degradable plastics derived from fossil fuel feed stocks, is constantly directing the research activities towards the investigation and use of different biopolymers in many potential applications, including food packaging (De Azeredo, 2009; Ruiz-Hitzky, 2013). However, these materials generally present low mechanical resistance and high sensitivity to environmental conditions. As a result, many attempts have been carried out to develop films based either on blends of different biopolymers or containing fillers (Rhim et al., 2013), natural based plasticizers (Vieira et al., 2011) and nanoreinforcements (Rhim and Ng, 2007), able to improve specific properties for packaging application purpose. Polyvinyl alcohol (PVA) is a water soluble and semi-crystalline plastic, widely utilized not only in food packaging, but also in some other applications, like biomedical, household and construction sectors, because of its excellent properties, including solvent resistance, mechanical performance and biocompatibility (Kubo and Kadla, 2003; Liu et al., 2014). Nevertheless, PVA has some drawbacks like low biodegradation rate and high moisture absorption. In order to improve its environmental eco-friendliness and performance, PVA is usually mixed with other biopolymers and/or biobased reinforcements: it has been utilized as matrix for nanocellulose (Fortunati et al., 2013a; Fortunati et al., 2013b; Ibrahim et al., 2010; Lee et al., 2009; Voronova et al., 2015), micro/nano lignin (Hu et al., 2016; Nair et al., 2014a; Xu et al., 2013), and it has been also blended with chitosan (Bonilla et al., 2014; Lee et al., 1996; Srinivasa et al., 2003).

Chitosan (CH), a copolymer of 2-glucosamine and N-acetyl-2-glucosamine units, is a polysaccharide isolated from crustacean shells, like crab and shrimp. It has been widely studied for application in biosensors, tissue engineering, separation film, water treatment, due to its excellent properties as antioxidant, antibacterial agent, and for its good biocompatibility and biodegradability (Crini and Badot, 2008; Kumar, 2000; Rinaudo, 2006). However, some disadvantages, such as dissolution in highly acidic solution, low surface area, high cost, poor thermal and mechanical properties, restrict its applications. It is expected that the combination of PVA with chitosan should have considerable effects on biological activities of the films, taking into consideration the good biological performance of neat chitosan. Studies on PVA/chitosan blend films have been reported in (Srinivasa et al., 2003), where the authors

studied how to modulate the chain flexibility of chitosan membrane for different specific purposes. Bonilla et al. (Bonilla et al., 2014) studied the blending of PVA with CH in different compositions to obtain biodegradable films (PVA:CH mass ratio of 90:10, 80:20 and 70:30). The structural, thermal, mechanical, barrier properties, as well as antimicrobial activity, were tested for neat PVA and blends. Results revealed that PVA and CH have good compatibility, but the chitosan induced a reduction of crystallinity of the blends. Moreover, addition of chitosan significantly reduced the film deformability and simultaneously increased the film rigidity, mainly at the ratio (70:30) of PVA:CH. Additional advantage of using chitosan coupled with PVA films is related to the possibility of both decreasing UV transmittance and providing, at the same time, antimicrobial activity. Abou-Aiad et al. (Abou-Aiad et al., 2006) used minimum inhibitory concentration (MIC) method to investigated the biological activities of PVA/CH against a representative number of pathogenic organisms. They found that the MIC for PVA/CH blend decreased with increasing amount of CH dose in the blends.

Lignin, which makes up 20-30% of the cell walls of plants, is the second most abundant natural polymer next to cellulose. It has always been utilized in low-value fields, for example heat and electricity generation. Nowadays, many researchers are realising that its abundance could not only potentially resolve the problem of rapid depletion of resources, but it could also gain higher value, reconsidering its use as antioxidant, UV absorbent, antimicrobial and reinforcement agent, carbon precursor and biomaterial for tissue engineering and gene therapy (Kai et al., 2016; Thakur et al., 2014).

Hu et al. (Hu et al., 2016) investigated PVA/modified lignin (eucalypt lignosulfonate calcium) composites, and showed that microlignin was homogenously dispersed in PVA matrix, due to the strong interactions. DSC results shave shown that only one T_g can be observed at the selected blend ratios, indicating a good miscibility. Thermogravimetric analysis also suggested that a very small amount (3 wt %) of lignin could significantly alter the thermal decomposition temperature of PVA. Actually, lignin nanoparticles (LNP) extracted from pristine alkali lignin by hydrochloric acidolysis, have shown to have more remarkable effects than the large particles at lower loading in biopolymeric nanocomposites, as reported in previous published works (Yang et al., 2015a; Yang et al., 2015b; Yang et al., 2015c). Looking again at the nanoscale, Nair et al. (Nair et al., 2014a) reported that nanolignin particles were more

effective than original lignin in increasing the thermal stability when used with polyvinyl alcohol,. Nair et al. (Nair et al., 2014b) also prepared and characterized a range of chitosan – alkali lignin composites to remove the harmful effluents (dyes and metal ions) present in waste water. Various parameters (chitosan content, initial pH and adsorbent dosage) were studied. Batch adsorption studies revealed that CH:lignin (50:50) composite exhibited maximum percentage removal of anthraquinonic dye, Remazol Brilliant Blue R and Cr(VI) compared to other cases. A recent study also reported the use of nanoparticles combining chitosan and lignosulfonates for cosmetic and biomedical uses (Kim et al., 2013). Greater stability to lysozyme degradation, antimicrobial activity and biocompatibility with human cells were obtained upon lignosulfonates incorporation into chitosan nanoparticles. However, no examples are available in the literature that approached the use of lignin based material at the nanoscale in chitosan or in PVA modified chitosan films.

According to this, in the present work lignin nanoparticles were introduced both in binary (PVA or chitosan) and ternary (PVA/chitosan (90:10) blend) nanocomposite systems with different weight loading by solvent casting approach. Thermal, mechanical, optical characterization, overall migration activity, and antiradical and antibacterial activity of the produced formulations towards two different plant/fruit pathogens were tested and here reported. This work may provide a new potential application for PVA and CH based nanocomposite films and their blends containing high-performing lignin nanoparticles in food packaging sector.

2 Experimental

2.1 Materials

Polyvinyl alcohol (PVA) (Mw 124–146 kg mol^{-1}, 99% hydrolysed) and high molecular weight chitosan (CH), (practical grade, Batch MKBB0585, degree of deacetylation >77%, viscosity: 1220 cPs, 1.61×10^5 Da), were supplied by Sigma–Aldrich. Pristine lignin, obtained as bio-residue of conversion of Arundo donax L. biomass to bioethanol in a steam explosion pre-treatment was supplied by CRB (Centro Ricerca Biomasse, University of Perugia) (Cotana et al., 2014). All the chemical reagents were supplied by Sigma–Aldrich® and used as received.

2.2 Methods

2.2.1 Preparation of binary PVA/LNP, CH/LNP and ternary PVA/CH/LNP nanocomposite films

LNP suspension was extracted from pristine lignin via hydrochloric (HCl) acidolysis, as reported in (Yang et al., 2015c). Binary nanocomposite formulations were prepared diluting PVA in millipore water at 1.5% (wt/wt) under magnetic stirring at 90 °C for 3 h., maintained up to reach room temperature (RT). After that, PVA solutions were mixed with different amount of LNP (0, 1 and 3 wt %, respectively) in aqueous suspensions and then sonicated (Vibracell 75043, 750 W, Bioblock Scientific) for 5 min at 40% of amplitude, obtaining films labelled as PVA, PVA/1LNP and PVA/3LNP.

Chitosan (0.15% wt/wt) was dissolved in water containing 1% v/v of glacial acetic acid under stirring for 12 h at 40 °C, after that the same procedure selected for PVA based films was considered, and nanocomposite films designed as CH, CH/1LNP and CH/3LNP, were produced. For the preparation of ternary PVA/CH/LNP nanocomposites, the films were prepared through mixing PVA and CH solutions at 90:10 mass ratio (on the basis of results from previous optimised studies) (Bonilla et al., 2014), followed by the same procedures applied for the realization of PVA/LNP based films. The resulted ternary composites were designed as PVA/CH, PVA/CH/1LNP and PVA/CH/3LNP, respectively (**Table 1**). The dispersions were cast in levelled polytetrafluorethylene (PTFE) Petri dishes (9 cm diameter, 15 g/solution per dish) and dried in the oven at 40 °C, at about 40% relative humidity (RH), for 1 day. The films were peeled off and stored in chambers with saturated $Mg(NO_3)_2$ solutions at either 53% RH 25°C, prior to all analyses.

2.2.2 Fourier-transform infrared (FT-IR) spectroscopy

FT-IR spectra were recorded using a Nicolet iS50 FT-IR spectrometer (Thermo Scientific) equipped with attenuated total reflectance accessory (ATR). The FT-IR spectra were measured at RT in the range of 400–4000 cm^{-1}. Measurements of absorbance were taken with DTGS KBr detector with 2 cm^{-1} resolution and 32 scans for each sample were averaged.

2.2.3 *Tensile properties*

According to the UNI ISO 527-1 standard, tensile tests of the films were carried out via a Universal Testing Machine (digital Lloyd instrument) to obtain the true stress-strain curves. Rectangular samples (1×5 cm^2) were prepared and conditioned at room temperature in a box with $Mg(NO_3)_2$ saturated solution (53% RH). Equilibrated film samples were fixed in the film-extension grips and stretched until breakage. A 500 N load cell and a 5 mm min^{-1}crosshead speed were used. The tests were performed at RT and at least six duplicates for each formula were measured. Tensile strength (□), Young modulus (E) and elongation at break (□$_b$) were evaluated.

2.2.4 *Differential scanning calorimetry (DSC)*

About 5 mg of film samples were tested by using a differential scanning calorimeter (DSC, TA Instrument, Q200). Measurements were performed in the range from -25 °C to 220 °C under nitrogen flow, at a heating rate of 10 °C/min. After the first heating step, cooling and second heating steps were also performed. Glass transition temperature (T_g), melting temperature (T_m) and melting enthalpy (□H_m) were determined, respectively, during the cooling and the 2nd heating scans. Three tests for each material were repeated. The cristallinity degree was calculated as:

$$\chi = \frac{\Delta H_m}{\Delta H_{m0}(1-m_f)} \times 100 \qquad (1)$$

where ΔH_m is the melting (or crystallization) enthalpy, ΔH_{m0} is the melting enthalpy for a 100% crystalline PVA, 161.6 J/g (Roohani et al., 2008) and (1 - m_f) is the PVA mass ratio in the measured samples.

2.2.5 *Thermogravimetric analysis (TGA)*

TGA tests were implemented through a thermo gravimetric analyzer (TGA, Seiko Exstar 6300). Approximately 8 mg of samples were heated from 30 to 700 °C under nitrogen atmosphere at a heating rate of 10°C/min. The weight-loss rate and maximum thermal degradation temperature (T_{max}) were collected from derivative thermogravimetric (DTG), together with the residue at 600 °C.

2.2.6 *Overall migration activity*

Considering the potential use of the PVA nanocomposite films in fresh food packaging fields, overall migration measurements were carried out in simulant D2 (isooctane). Based on the European Standard EN 1186-1/2002, rectangular strips of 10 cm^2 in 10 mL of food simulants were utilized. Samples were maintained in the isooctane solution in standard conditions for 2 days at 20 °C. After finishing the incubation, films were removed out and the simulants were poured into glass dishes and evaporated. The migration value (mg kg^{-1}) of the simulant was determined by weighing the residues with an analytical balance (±0.01 mg precision).

2.2.7 *Antiradical activity of migrating substances*

DPPH radical scavenging activity for PVA and chitosan films containing lignin nanoparticles was determined on the basis of the method reported by Byun et al. (Byun et al., 2010) and Domenek et al. (Domenek et al., 2013)], with a slight modification. Film (0.1 g) was cut into small pieces and immersed in 2 mL of methanol for 24 h at ambient temperature. The obtained supernatant was collected for evaluation of DPPH radical scavenging activity: methanol extract (1 mL) was mixed with DPPH in methanol (1 mL, 50 mg/L^{-1}), resulting in a 25 mg/L^{-1} DPPH concentration solution. The mixture was maintained at RT in darkness for 1 h. Absorbance values at 517 nm were taken by using a UV-Vis spectrometer (Varian, Cary 4000). The mixture solution of methanol extracted from neat PVA and DPPH methanol was used as control. DPPH radical scavenging activity was calculated by Equation 2, where A_{sample} was the absorbance of sample and $A_{control}$ was the absorbance of the control.

$$(RSA,\%) = \left[\frac{A_{control} - A_{sample}}{A_{control}} \right] * 100 \qquad (2)$$

2.2.8 *Colour test and optical properties*

Colour variation was investigated with a spectrophotometer (CM-2300d Konica Minolta). Data were collected by using the SCI 10/D65 approach. CIELAB colour variables, defined by the Commission Internationale de 1′Éclairage (CIE 1995) (CIE, 1995), were considered. Film samples were placed on a white standard plate and *L**, *a**, and *b** values were determined. *L**

(0-100) indicates tendency towards whiteness; *a** (-80-100) indicates tendency from greenness towards redness and *b** (-80-70) indicates tendency from blueness towards yellowness. Three measurements were randomly taken on each film, Δ*E*, defined as the colour difference among films, was also calculated, as indicated in Equation (3), designing PVA as control:

$$\Delta E = \sqrt{(\Delta L^*)^2 + (\Delta a^*)^2 + (\Delta b^*)^2} \quad (3)$$

The colour tests were additionally verified using a Varian (Cary 5000) UV-Vis spectrometer equipped with an integrating sphere. Data were presented in CIE1931 colour variables.

Light transmittance of the PVA nanocomposite films was tested via a Varian UV-Vis spectrometer (Cary 4000). The scan from 250 to 900 nm was performed at 240 nm/min speed, thickness of all samples were normalized as 20 μm in the test.

2.2.9 Microstructure

Morphology of the cross-sections of the PVA films was analyzed via a Field Emission Scanning Electron Microscope (FESEM) Supra 25-Zeiss. Film specimens were cryo-fractured in liquid nitrogen and the surface was then gold coated. Observation was performed by using an accelerating voltage of 5 kV.

2.2.10 Antibacterial activity

Biocidal activity of neat PVA, CH, PVA/CH films and nanocomposites containing lignin nanoparticles was evaluated against *Xanthomonas arboricola* pv. *pruni* (Xap - 3894) and *Pectobacterium carotovorum* subsp. *odoriferum* (Pco - 1115) bacterial plant pathogens. Both bacteria are able to cause damages to fresh fruits/vegetables in open field and during post-harvest phases. In particular, Pco - 1115 is especially dangerous, due to its ability to develop severe soft rot, determining relevant economic losses on fresh vegetables and stored fruits (Waleron et al., 2014). Xap - 3894 is a quarantine bacterial plant pathogen, responsible for damages to different organs and fresh fruits of several *Prunus* spp. (almond, peach, cherry, plum, apricot). The antibacterial activity of binary and ternary nanocomposite films containing 3 wt % of LNP (the highest content of LNP used in the present work) was evaluated with

respect of Pco -1115 and Xap -3894 phytobacteria, utilized at an initial concentration of 1 x 10^6 CFU/mL. The experiments were carried out using Nutrient Broth (NB) 4% by the liquid medium test (Schaad et al., 1988). The different thesis (PVA/3LNP, CH/3LNP and PVA/CH/3LNP) consisted in 3 replicates each and 5 sterile glass tubes per thesis, each tube containing 5 mL of liquid broth (NB) with 1 x 10^6 CFU/mL of Xap - 1115 and Pco - 3894 and the various nanocomposite film samples (3.24 cm^2). Neat PVA, CH and PVA/CH based films were also tested as control. All tubes were placed on a reciprocal shaker for 48 h at 25 ± 2 °C at 150 rpm. Samplings from all tubes/thesis were carried out at 0, 1, 3, 12 and 24 h (after bacterial inoculation) and serial dilution were carried out and plated on NAS. After 48 h at 26 ± 1 °C the number of Pco -1115 and Xap -3894 bacterial colonies were counted. All data were statistically elaborated using GraphPad Prism 4 software by analysis of variance (ANOVA) and significance of treatments was determined using Tukey's HSD test ($P \leq 0.05$). (Steel and JH Dickey, 1997).

3 Results

3.1 FT-IR analysis

The intermolecular interactions between PVA, chitosan and lignin nanoparticles were investigated by FT-IR spectroscopy. The results for PVA/3LNP, CH/3LNP and PVA/CH/3LNP systems are reported in **Figure 1a-c**, respectively. The spectrum of neat PVA shows some absorption peaks potentially sensitive to intermolecular interactions. These are bands at 3262 cm^{-1}, assigned to the stretching of OH group, 1077 cm^{-1} and 1412 cm^{-1} related to C–O bonds (Kanimozhi et al., 2016). Lignin nanoparticles in PVA matrix leads to intensity variation of mentioned bands, which could be ascribed to the interaction between –OH group on the LNP surface and the hydroxyl groups of the PVA matrix. Moreover, changes in the shape of bands at 846 cm^{-1} and 2900-2950 cm^{-1} may be assigned to the conformational changes of PVA chains. Lack of lines at wavenumbers higher than 1700 cm^{-1} proves high degree of deacetylation of PVA. Slight modifications in intensity of some peaks, related to the presence of lignin nanoparticles, are also visible at 1648 cm^{-1} (water absorption) and C−C stretching of aromatic skeleton (at 1566 cm^{-1}).

The FT-IR spectrum of pure CH exhibits the characteristic IR peaks of $NHCOCH_3$ at 1632 cm^{-1} (amide I band) and NH_2 at 1546 cm^{-1} (amide II band) (Vicentini et al., 2010) that were not modified in intensity and wavenumber when LNP were introduced. In the case of PVA/CH blend, the two main characteristic peaks related to CH were shifted towards higher wavenumbers (at 1637 cm^{-1} and at 1550 cm^{-1}, respectively), due to the interaction between OH and NH bending vibration in PVA/CH, while no shift has been detected for PVA peak measured at 1316 and 1412 cm^{-1}. Compared to the spectra of PVA/CH film, some differences were found in the case of ternary systems: the bands at 3261 cm^{-1} and 1086 cm^{-1} are shifted towards lower wavenumber values (3251 and 1080 cm^{-1}, respectively) in the PVA/CH/3LNP. These shifts result from a formation of intermolecular hydrogen bonds among the OH of PVA, OH, NH of CH and OH of LNP. The FT-IR spectra of ternary system (PVA/CH/LNP) also show an increase in the absorbance of the band at 1559 cm^{-1}: the decreased intensity ratio of this band and 1423 cm^{-1} band with the presence of LNP indicates that interactions are established between LNP and PVA O-H groups.

3.2 Tensile characterization

Food packaging films are required to maintain their integrity to withstand the stress that occurs during handling, storage and shipping (Kanatt et al., 2012), so tensile tests were performed to evaluate the effects of LNP dose and its combination with PVA and chitosan on the elastic-plastic response of the final produced nanocomposites. The results are reported in **Figure 2** (from 2a to 2c). Typical stress-strain curves acquired from the tensile tests are exhibited in **Figure 2d**. When binary PVA system loaded with LNP are considered, it is observed that LNP gives an significant contribution to mechanical performance of the nanocomposites, with an increase of the Young's modulus from 1100 to 2100 MPa when 3 wt % of LNP was incorporated in PVA matrix, along with the increase in tensile strength from 45.8 to 51.5 MPa, 91% and 12.4% higher than those of pure PVA. In the meanwhile, the elongation at break decreased from 163.4 to 115.5% and 30.5%, respectively for PVA/1LNP and PVA/3LNP nanocomposites, while the PVA film exhibited a typical ductile behaviour. Kuko et al. (Kubo and Kadla, 2003) reported the calculation of interaction energy density of -9.34 cal cm^{-1} for PVA and lignin, suggesting that strong intermolecular (interfacial) interactions

form between PVA and lignin, as confirmed by FT-IR analysis. Although the PVA/lignin system is immiscible, the results showed the existence of some specific intermolecular interactions between PVA and lignin. The same results were also confirmed by Korbag et al. (Korbag and Mohamed Saleh, 2016), who used nuclear magnetic resonance and FTIR spectroscopy techniques. Recently, Ye et al. (Ye et al., 2016) and Hu et al. (Hu et al., 2016) also reported that PVA/lignosulfonate films had preferable mechanical properties than pure PVA film, due to the primary rigidity of lignin structures and the formation of strong hydrogen bonds.

In binary chitosan based systems, CH films proved to be the least stretchable, as opposed to those of PVA. LNP addition did not improve the tensile strength, the modulus even decreased from 1334 (CH) to 995 MPa (CH/3LNP). However, the elongation at break increased gradually from 5.72 to 17.31% with increase in LNP loading. Actually, this toughness effect of lignin has also been reported before in other polymer systems (Mu et al., 2014; Sun et al., 2015; Yang et al., 2015b), which could be attributed to the good dispersion of LNP in CH.

In ternary PVA/CH/LNP system, the addition of CH induced an important decrease of tensile strength and Young's modulus. The results demonstrated that CH has not a reinforcement effect on PVA matrix, which was consistent with previous study (Bonilla et al., 2014). Elongation at break gives information about the film flexibility and deformability: in our specific case, the ternary systems still maintain a ductile behaviour and the deformability of the system is recovered with 3% wt. of LNP (PVA/CH/3LNP film keeps the same level as pure PVA film, while the elongation at break was reduced from 163.4 to 92.9 when 10 wt % of chitosan was added to neat PVA). The mechanism is not very clear, but it is worth to note that the enhanced elongation at break of neat PVA in presence of LNP and chitosan could be ascribed to the flexibility of the special lignin structure, in which ether linkages link with benzene rings that served as internal plasticizers) (Wang et al., 2012).

3.3 Thermal analysis

DSC analysis was utilized to analyze the thermal performance of PVA, CH and LNP binary and ternary system nanocomposites in relation to their composition. The thermal parameters detected in the first heating, cooling and second heating scans for all films are summarized in

Table 2, while DSC cooling and 2nd heating curves for PVA/LNP and PVA/CH/LNP, cooling scan for CH/LNP nanocomposite films are reported, in **Figure 3a**, **Figure 3b** and **Figure 3c,** respectively.

For pure PVA, T_g occurs at 84.6 °C and slightly shifts up to 86.9 °C when 3 wt % of LNP was incorporated (**Table 2**) (Nishio and Manley, 1988). This is due to the polymer interactions through the hydrogen bond formation. PVA is a semicrystalline polymer contaniing lots of hydroxyl groups which form inter- and intra-molecular hydrogen bonds. Since LNP also have a lot of hydroxyl groups in its structures, strong molecular interactions (like hydrogen bonding or dipole-dipole interactions) between the polymer and LNP can be expected (Hu et al., 2016; Kubo and Kadla, 2003; Ye et al., 2016). Binary PVA systems also showed higher crystallization temperature (T_c) by about 25°C in comparison with neat PVA (T_c = 201.0±0.1 °C for PVA/3LNP, while the neat PVA registered a value of 177.6±1.2 °C) (**Figure 3a**). This result evidences that LNP are able to enhance the crystallization of the PVA by acting as heterogeneous nucleating agents. Consequently, a notable enhancement of T_m values of PVA during the 2nd heating scan was registered with LNP loading (**Table 2**), due to reduced mobility of PVA chains. In the meanwhile, PVA/1LNP and PVA/3LNP nanocomposites exhibit narrower endothermic peak than PVA at about 220–230°C, as shown in **Figure 3b**, corresponding to the melting of the crystalline phase of PVA. The calculated percentage of cristallinity is also shown in **Table 2**, where the cristallinity X_c of PVA increased to 18.1 % (PVA/3LNP) from 9.8 % (PVA) when the LNP value increased in the blend, clearly evidencing how well dispersed LNP could be serve as nucleation agents in PVA, so supporting the results of mechanical characterization.

In the case of CH/LNP binary films, chitosan did not show significant variations in the selected temperature range after the 1st and 2nd heating scans (not reported in the present study). During the cooling procedure, modification of the exothermic curves at the T_g could be visible in the temperature range of 135-115 °C (**Figure 3c**). The addition of 3 wt % LNP induced a T_g reduction from 131.2 to 123.1°C, demonstrating that LNP lead to weaken the interactions (like hydrogen bond) between chitosan macromolecules.

In the case of PVA/CH blend, the mixture effect of compatible polymers on T_m implies that its values are intermediate between the respective pure polymers, in agreement with measured

values for pure PVA (Bonilla et al., 2014) and CH (Kittur et al., 2002; Sakurai et al., 2000). A less notable increase of T_m in ternary systems, with respect to PVA/LNP binary system films, was observed: as in the case of PVA/LNP binary system films, the cristallinity values for LNP containing PVA/CH blend were also increased, probably due to the higher weight percentages of LNP in PVA matrix (LNP account for 1.11 and 3.33 % of PVA weight in cases of PVA/CH/1LNP and PVA/CH/3LNP, respectively).

In order to investigate the effect of LNP loading on the thermal degradation behaviour of resulted composites, TG and DTG curves of pure PVA, CH and LNP binary and ternary systems were recorded (**Figure 4a** and **Figure 4b**). The peak values of DTG and the residual weight at 600 °C, were also summarized in **Table 3**. The small weight loss at 75-100 °C (about 10%) is due to the loss of adsorbed, bound water and residual acetic acid. The maximum weight loss (peak 2) at 200-300 °C was attributed to the thermal degradation of CH and PVA. The third weight loss step at 400-450 °C is related to the PVA main thermal degradation event (Bonilla et al., 2014; Chen et al., 2008). Evidently, with increasing the dose of LNP from 0 to 3 wt %, the peak 1 shifted from 85.0 up to 95.3°C for PVA/LNP binary system films, from 59.2 to 79.4°C for CH/LNP binary system films and from 82.3 to 98.4°C for PVA/CH/LNP ternary system films. This shift can be attributed to improved barrier property of well dispersed LNP in PVA and/or CH, that efficiently delayed the removal of water and residual acetic acid. Similar results were observed in our previous study with wheat gluten in presence of glycerol (Yang et al., 2015c). On the other hand, the peak 2 value of PVA/CH film was 249.1 °C, about 9 °C lower than that of neat PVA film, which confirmed that CH did not improve the thermal resistance of PVA. When the LNP was used, these peak 2 values remarkably increased to 278.6 (PVA/3LNP) and 277.8 °C (PVA/CH/3LNP), respectively. It is worthwhile to note that the addition of LNP seemed not to increase the degradation temperature of CH. However, the addition of low content of LNP seemed not to influence the residual weight of the nanocomposites. Consequently, the increasing two peak temperature values indicate that the PVA films showed slightly enhanced thermal stability due to the LNP addition.

3.4 Antiradical activity of migrating substances

In order to actively protect the packaging towards oxidation, two strategies are often employed, such as the design of active compound releasing systems and the inclusion of scavenging systems (Nerin et al., 2008). In this latter case, one simple method can be considered for measurement of radical scavenging activity in the case of polymer films: DPPH assay shows how DPPH decolorizes, as a result of reduction in absorbance values, in presence of antioxidants (Enayat and Banerjee, 2009). The antioxidants reduce the DPPH radicals to a yellow-coloured compound, diphenylpicrylhydrazine, and the reaction extent relies on the hydrogen-donating ability of the antioxidants (Blois, 1958; Siripatrawan and Harte, 2010).

Figure 5 (a and **b)** and **Table 4** show the antioxidant response of migrating substances for different nanocomposite films directly immersed into the methanol solution for 24 h. The pure PVA samples were regarded as control samples and did not show any DPPH radical scavenging activity, as expected. When incorporating 1 wt % of LNP, the absorption value at 517 nm of PVA/1LNP film decreased to 0.103 from 0.4724, while RSA value increased to 78.2%, highlighting a noticeable antioxidation response. When the dose of LNP raised up to 3 wt % (PVA/3LNP film), a more remarkable DPPH scavenging activity could be obtained (89.0%). Antioxidant properties of chitosan derivatives have been studied (Kim and Thomas, 2007; Xie et al., 2001). Compared with PVA film, chitosan film without LNP filler exhibited some scavenging activity on DPPH (20.3%). The scavenging mechanism of chitosan is based on the fact that the residual free amino (NH_2) groups can react with free radicals to form stable macromolecule radicals, afterwards NH_2 groups form ammonium (NH_3^+) groups by absorbing the hydrogen ions from the solution (Yen et al., 2008). In the films containing 3 wt % LNP (CH/3LNP), the antioxidant activity increased more than 4.5 folds in relation to the CH samples. It should be noted that in the ternary systems, the antioxidant activity was more correspondingly evident than in binary systems, since higher RSA values (24.3, 85.6 and 91.7 % for PVA/CH, PVA/CH/1LNP and PVA/CH/3LNP, respectively) could be obtained.

3.5 Overall migration activity

Overall migration test with food simulant D2 (isooctane) was performed and the results are summarized in **Figure 6**. The idea was to examine the potential use of these nanocompo-

site films in the fatty food packaging. After incubation for 2 days at 20 °C in isooctane solution, the maximum migration level was 30.5 mg kg^{-1} of simulant measured for the PVA/CH/3LNP material. This value is well below the migration legislative limits for food contact materials (60 mg kg^{-1}, or 10 mg dm^2) simulant, established by the current European legislation. The migration level increased with increasing loading amount of LNP in the resulted binary and ternary films: the migrated substances should contain more free lignin nanoparticles, as confirmed by the improved anti-oxidation activity of nanocomposites containing 3 wt % of LNP (i.e. PVA/3LNP, CH/3LNP and PVA/CH/3LNP) (see results of section 3.4) (Yang et al., 2016).

3.6 Colour and optical properties

The effects of LNP dose on film colour and opacity are shown in **Figure 7** and **Table 5**. Adding LNP into PVA and chitosan films significantly affected *L**, *a** and b* values of the film surface. Films without LNP have higher *L** value, while *L* val*ues of the binary PVA films varied from 92.03 to 64.92; *a** increased from 3.36 to 8.64 (indicating tendency towards redness), *b** values increased from 13.71 to 61.98 (indicating tendency towards brownish), Δ*E* value went up to 55.62 when the LNP loading increased from 0 to 3 wt.%. The same tendency could be also observed in binary CH/LNP and PVA/CH/LNP ternary films. It is also worthy to look at the colours of prepared composites shown in CIE 1931 space chromaticity diagram (Fig. 7a). It is clear that a tendency of colour changes, induced by presence of LNP is the same for all materials, as it is marked by arrow in Fig.7a.

UV light resistance is strictly required to be considered when polymeric films are considered in packaging, especially in the case of light-sensitive food products (Auras et al., 2004). Although PVA is widely applied as a packaging material, its poor UV resistance needs to be improved in order to broaden the application sector. LNP have showed excellent UV barrier property in our previous studies (Yang et al., 2015a; Yang et al., 2015b; Yang et al., 2015c). It can be also commented that the transmittance of the previous studied nanocomposite films (Figure 7a) containing LNP in the UV region (for instance 320 nm) reached value below 2 % (**Table 4**), confirming how these nanocomposites could be used in specific fields where UV protection is needed. On the other hand, PVA, chitosan and their blend films

without LNP were more transparent (lower transmittance value at 550 nm in **Table 4**) than those coupled with LNP. The opacity of the films significantly increased with increasing LNP content.

3.7 Microstructure

Figure 8 presents the FESEM micrographs illustrating the cross section morphology of PVA, CH and PVA/CH/LNP based films. The FESEM micrograph of pure PVA shows a smooth surface. For PVA/1LNP and PVA/3LNP films, the LNP agglomerates can be observed along with the well dispersed lignin nanoparticles in PVA matrix. Although the surface of them is rougher than pure PVA, a very good interfacial adhesion is evidenced between lignin and PVA, which contributed remarkable improvements in tensile strength and modulus discussed in the mechanical properties section (3.2). For chitosan based films, a different surface morphology was seen with respect to PVA based films. A very good interfacial adhesion is evidenced between lignin and chitosan, however cavity and agglomerates are observed with increasing content of lignin particles in chitosan matrix (Chen et al., 2009). PVA/CH film shows a continuous, homogeneous phase without any evidence of phase separation. Moreover, no irregularities, such as air bubbles, pores, cracks or droplets were detected. This indicates the high compatibility of the two polymers, as previously observed (Bonilla et al., 2014). The addition of LNP increased the toughness and agglomerate dots of resulted ternary films, but still maintaining an excellent interfacial adhesion.

3.8 Antibacterial activity

The antibacterial tests against two plant/fruit pathogens were implemented to evaluate the effect of both chitosan and LNP (used at the highest content) as possible active agents in a food active packaging solution. The results of bacterial growth confirmed that, in the case of Pco - 1115 growth, its multiplication was similar to control thesis even when it was placed in association with neat PVA, CH and PVA_CH films. Differently, bacterial development was significantly reduced in thesis with PVA/3LNP, PVA/CH/3LNP and CH/3LNP films. In particular after 3h, the greatest Pco - 1115 reduction was recorded by CH/3LNP film with values of 6.8 x 10^5 CFU/mL and the antibacterial activity of this film resulted effective over time by

a remarkable Pco - 1115 growth reduction also after 12 h (**Figure 9a**). Respect to *Xap - 3894* development, its growth resulted lower (after 3h) for control thesis and similarly when it was placed with PVA, CH and PVA_CH films. On the other hand, due to the antibacterial properties of PVA/3LNP, PVA/CH/3LNP and CH/3LNP films, Xap -3894 development was observed. In particular, the antibacterial activity of PVA/CH/3LNP film allowed to obtain a remarkable reduction of Xap - 3984 growth. After the artificial bacterial inoculum, Xap - 3894 values recorded were equal to 4.1 x 10^5 CFU/mL, 9.8 x 10^5 CFU/mL, 2.6 x 10^7 CFU/mL and 9.7 x 10^7 CFU/mL, after 1, 3, 12, 24 h, respectively, always lower to the values recorded by all the other thesis (**Figure 9b**).

Bacterial plant pathogens included and tested in this study have represented a valid point of reference to evaluate the antibacterial activity of the developed nanocomposite films. Pco - 1115 and Xap - 3894 represent practical examples of damages and losses during post-harvest of fresh fruits and vegetables (2006; Toth et al., 2003). Binary (PVA/3LNP and CH/3LNP films) and ternary nanocomposite systems (PVA/CH/3LNP blend) showed a remarkable antibacterial activity in respect to both Pco - 1115 and Xap - 3894 phytobacteria. In particular, the films containing both chitosan and lignin nanoparticles (PVA/CH/3LNP and CH/3LNP) revealed the capacity to maintain this activity over the time. The results confirmed that the developed nanocomposite systems represent an innovative and sustainable strategy for different packaging films chains, to preserve as well as to better successfully maintain food products.

4 Conclusions

Thermal, optical, mechanical properties, migration, antioxidant and antibacterial activities as well as morphologies of binary and ternary polymeric films based on polyvinyl alcohol (PVA), chitosan (CH) and lignin nanoparticles (LNP) at two different amounts (1 and 3 wt %) were investigated. The morphology studies showed that a relatively good dispersion and an excellent interfacial adhesion was achieved between LNP and PVA, CH and PVA/CH blend, which contributed to remarkable improvements in the mechanical performance. Tensile results revealed that the addition of LNP enhanced the tensile strength and modulus for PVA, and induced a toughness effect in CH matrix. LNP served both as nucleation agents in PVA and barrier, notably delaying the thermal degradation of binary and ternary systems nano-

composites. It can be also commented that the transmittance of the studied nanocomposite films containing LNP in the UV region (for instance 320 nm) reached values below 2 %, illustrating these nanocomposite films could be used where UV protection is necessary. In addition, LNP and CH proved to have a synergistic antioxidation response, observed on the basis of band disappearance at 517 nm for the free radical 2,2-diphenyl-1-picrylhydrazyl (DPPH). Overall migration test shows that the migration level is well below the legislative limits (60 mg kg^{-1} simulant) for food contact materials in the case of fatty foods. Moreover, antimicrobial tests revealed a capacity to inhibit the Gram negative bacterial growth of *Erwinia carotovora subsp. carotovora* and *Xanthomonas arboricola pv. pruni* along the time, offering innovative opportunities against dangerous bacterial plant/fruit pathogens. Concluding, the results underlined the possibility to use the proposed formulations as potential novel food contact materials for both fatty and fresh products suggesting their possible application as active packaging formulations.

Acknowledgements

Weijun Yang appreciates the funding support from China Scholarship Council (CSC).

Figure and Tables captions

Figure 1: FTIR spectra of PVA/3LNP, CH/3LNP and PVA/CH/3LNP systems.

Figure 2: Tensile strength (a), Young's modulus (b), elongation at break (c) and stress-strain curves (d) of PVA, CH and PVA/CH/LNP nanocomposites.

Figure 3: DSC curved of first heating (a), second heating (b) and cooling scans (c) of PVA, CH and PVA/CH/LNP nanocomposites.

Figure 4: TG (a) and DTG curves (b) of neat PVA, CH and LNP binary and ternary nanocomposites

Figure 5: Antioxidant activities of migrating substances for different PVA nanocomposite films immersed directly in the methanol solution for 24 hs: monitoring of the absorbance for band at 517 nm (a) and colour variation of the DPPH methanol solution (b).

Figure 6: Overall migration in isooctane for PVA, CH and PVA/CH/LNP nanocomposites.

Figure 7: Effects of LNP dose on film colour and opacity (a) and UV–Vis spectra of binary

and ternary PVA nanocomposite films (b).

Figure 8: FESEM cross section micrographs of PVA, CH and PVA/CH/LNP nanocomposites.

Figure 9: (a) Antibacterial activity of different films based on PVA, CH and PVA/CH/LNP nanocomposites, on the multiplication of plant pathogenic bacteria *Pectobacterium carotovorum* subsp. *odoriferum (Pco) (CFBP 1115)* 1×10^6 CFU/mL; (b) Antibacterial activity of different films based on PVA, CH and PVA/CH/LNP nanocomposites, on the multiplication of plant pathogenic bacteria *Xanthomonas arboricola* pv. *pruni (Xap) (CFBP 3894)* 1×10^6 CFU/mL.

Table 1: Binary and ternary nanocomposite formulations

Table2: Thermal parameters derived from DSC analysis of PVA, CH and PVA/CH/LNP nanocomposites

Table 3: TGA results of PVA, CH and PVA/CH/LNP nanocomposites

Table 4: Optical properties and antioxidation activity of the migrating substances for PVA, CH and PVA/CH/LNP nanocomposites

Table 5: Results of color test for PVA, CH and PVA/CH/LNP nanocomposites

References

- 2006. Xanthomonas arboricola pv. pruni. Bulletin OEPP/EPPO Bulletin 36, 129-133.
- Abou-Aiad, T.H.M., Abd-El-Nour, K.N., Hakim, I.K., Elsabee, M.Z., 2006. Dielectric and interaction behavior of chitosan/polyvinyl alcohol and chitosan/polyvinyl pyrrolidone blends with some antimicrobial activities. Polymer 47, 379-389.
- Auras, R., Harte, B., Selke, S., 2004. An overview of polylactides as packaging materials. Macromolecular bioscience 4, 835-864.
- Blois, M.S., 1958. Antioxidant determinations by the use of a stable free radical.
- Bonilla, J., Fortunati, E., Atarés, L., Chiralt, A., Kenny, J.M., 2014. Physical, structural and antimicrobial properties of poly vinyl alcohol–chitosan biodegradable films. Food Hydrocolloids 35, 463-470.

572 – Byun, Y., Kim, Y.T., Whiteside, S., 2010. Characterization of an antioxidant polylactic
573 acid (PLA) film prepared with α-tocopherol, BHT and polyethylene glycol using film cast
574 extruder. Journal of Food Engineering 100, 239-244.
575 – Chen, C.-H., Wang, F.-Y., Mao, C.-F., Liao, W.-T., Hsieh, C.-D., 2008. Studies of
576 chitosan: II. Preparation and characterization of chitosan/poly (vinyl alcohol)/gelatin
577 ternary blend films. International journal of biological macromolecules 43, 37-42.
578 – Chen, L., Tang, C.-y., Ning, N.-y., Wang, C.-y., Fu, Q., Zhang, Q., 2009. Preparation and
579 properties of chitosan/lignin composite films. Chinese Journal of Polymer Science 27,
580 739-746.
581 – CIE, 1995. Industrial colour-difference evaluation. Technical report 116/1995 ed.
582 Commission Internationale de I'Eclairage Central Bureau, Wien, Austria.
583 – Cotana, F., Cavalaglio, G., Nicolini, A., Gelosia, M., Coccia, V., Petrozzi, A., Brinchi, L.,
584 2014. Lignin as co-product of second generation bioethanol production from
585 ligno-cellulosic biomass. Energy Procedia 45, 52-60.
586 – Crini, G., Badot, P.-M., 2008. Application of chitosan, a natural aminopolysaccharide, for
587 dye removal from aqueous solutions by adsorption processes using batch studies: A review
588 of recent literature. Progress in Polymer Science 33, 399-447.
589 – De Azeredo, H.M., 2009. Nanocomposites for food packaging applications. Food
590 Research International 42, 1240-1253.
591 – Domenek, S., Louaifi, A., Guinault, A., Baumberger, S., 2013. Potential of lignins as
592 antioxidant additive in active biodegradable packaging materials. Journal of Polymers and
593 the Environment 21, 692-701.
594 – Enayat, S., Banerjee, S., 2009. Comparative antioxidant activity of extracts from leaves,
595 bark and catkins of Salix aegyptiaca sp. Food Chemistry 116, 23-28.
596 – Fortunati, E., Luzi, F., Puglia, D., Terenzi, A., Vercellino, M., Visai, L., Santulli, C.,
597 Torre, L., Kenny, J., 2013a. Ternary PVA nanocomposites containing cellulose
598 nanocrystals from different sources and silver particles: Part II. Carbohydrate polymers 97,
599 837-848.
600 – Fortunati, E., Puglia, D., Monti, M., Santulli, C., Maniruzzaman, M., Kenny, J.M., 2013b.
601 Cellulose nanocrystals extracted from okra fibers in PVA nanocomposites. Journal of

602 Applied Polymer Science 128, 3220-3230.
603 – Hu, X.-Q., Ye, D.-Z., Tang, J.-B., Zhang, L.-J., Zhang, X., 2016. From waste to functional
604 additives: thermal stabilization and toughening of PVA with lignin. RSC Advances 6,
605 13797-13802.
606 – Ibrahim, M.M., El-Zawawy, W.K., Nassar, M.A., 2010. Synthesis and characterization of
607 polyvinyl alcohol/nanospherical cellulose particle films. Carbohydrate Polymers 79,
608 694-699.
609 – Kai, D., Tan, M.J., Chee, P.L., Chua, Y.K., Yap, Y.L., Loh, X.J., 2016. Towards
610 lignin-based functional materials in a sustainable world. Green Chemistry.
611 – Kanatt, S.R., Rao, M.S., Chawla, S.P., Sharma, A., 2012. Active chitosan–polyvinyl
612 alcohol films with natural extracts. Food Hydrocolloids 29, 290-297.
613 – Kanimozhi, K., Basha, S.K., Kumari, V.S., 2016. Processing and characterization of
614 chitosan/PVA and methylcellulose porous scaffolds for tissue engineering. Materials
615 Science and Engineering: C 61, 484-491.
616 – Kim, K.W., Thomas, R., 2007. Antioxidative activity of chitosans with varying molecular
617 weights. Food Chemistry 101, 308-313.
618 – Kim, S., Fernandes, M.M., Matamá, T., Loureiro, A., Gomes, A.C., Cavaco-Paulo, A.,
619 2013. Chitosan–lignosulfonates sono-chemically prepared nanoparticles: Characterisation
620 and potential applications. Colloids and Surfaces B: Biointerfaces 103, 1-8.
621 – Kittur, F.S., Harish Prashanth, K.V., Udaya Sankar, K., Tharanathan, R.N., 2002.
622 Characterization of chitin, chitosan and their carboxymethyl derivatives by differential
623 scanning calorimetry. Carbohydrate Polymers 49, 185-193.
624 – Korbag, I., Mohamed Saleh, S., 2016. Studies on the formation of intermolecular
625 interactions and structural characterization of polyvinyl alcohol/lignin film. International
626 Journal of Environmental Studies, 1-10.
627 – Kubo, S., Kadla, J.F., 2003. The formation of strong intermolecular interactions in
628 immiscible blends of poly (vinyl alcohol)(PVA) and lignin. Biomacromolecules 4,
629 561-567.
630 – Kumar, M.N.R., 2000. A review of chitin and chitosan applications. Reactive and
631 functional polymers 46, 1-27.

632 – Lee, S.-Y., Mohan, D.J., Kang, I.-A., Doh, G.-H., Lee, S., Han, S.O., 2009. Nanocellulose
633 reinforced PVA composite films: effects of acid treatment and filler loading. Fibers and
634 Polymers 10, 77-82.
635 – Lee, Y.M., Kimt, S.H., Kimt, S.J., 1996. Preparation and characteristics of β-chitin and
636 poly (vinyl alcohol) blend. Polymer 37, 5897-5905.
637 – Liu, P., Chen, W., Liu, Y., Bai, S., Wang, Q., 2014. Thermal melt processing to prepare
638 halogen-free flame retardant poly (vinyl alcohol). Polymer Degradation and Stability 109,
639 261-269.
640 – Mu, C., Xue, L., Zhu, J., Jiang, M., Zhou, Z., 2014. Mechanical and thermal properties of
641 toughened poly (L-lactic) acid and lignin blends. BioResources 9, 5557-5566.
642 – Nair, S.S., Sharma, S., Pu, Y., Sun, Q., Pan, S., Zhu, J., Deng, Y., Ragauskas, A.J., 2014a.
643 High Shear Homogenization of Lignin to Nanolignin and Thermal Stability of
644 Nanolignin- Polyvinyl Alcohol Blends. ChemSusChem 7, 3513-3520.
645 – Nair, V., Panigrahy, A., Vinu, R., 2014b. Development of novel chitosan–lignin
646 composites for adsorption of dyes and metal ions from wastewater. Chemical Engineering
647 Journal 254, 491-502.
648 – Nerin, C., Tovar, L., Salafranca, J., 2008. Behaviour of a new antioxidant active film
649 versus oxidizable model compounds. Journal of food Engineering 84, 313-320.
650 – Nishio, Y., Manley, R.J., 1988. Cellulose-poly (vinyl alcohol) blends prepared from
651 solutions in N, N-dimethylacetamide-lithium chloride. Macromolecules 21, 1270-1277.
652 – Rhim, J.-W., Ng, P.K., 2007. Natural biopolymer-based nanocomposite films for
653 packaging applications. Critical reviews in food science and nutrition 47, 411-433.
654 – Rhim, J.-W., Park, H.-M., Ha, C.-S., 2013. Bio-nanocomposites for food packaging
655 applications. Progress in Polymer Science 38, 1629-1652.
656 – Rinaudo, M., 2006. Chitin and chitosan: Properties and applications. Progress in Polymer
657 Science 31, 603-632.
658 – Roohani, M., Habibi, Y., Belgacem, N.M., Ebrahim, G., Karimi, A.N., Dufresne, A., 2008.
659 Cellulose whiskers reinforced polyvinyl alcohol copolymers nanocomposites. European
660 Polymer Journal 44, 2489-2498.
661 – Ruiz-Hitzky, E., 2013. Progress in Bionanocomposites: From green plastics to biomedical

applications.

– Sakurai, K., Maegawa, T., Takahashi, T., 2000. Glass transition temperature of chitosan and miscibility of chitosan/poly(N-vinyl pyrrolidone) blends. Polymer 41, 7051-7056.

– Schaad, N.W., Jones, J.B., Chun, W., 1988. Laboratory guide for identification of plant pathogenic bacteria. APS press St. Paul, MN.

– Siripatrawan, U., Harte, B.R., 2010. Physical properties and antioxidant activity of an active film from chitosan incorporated with green tea extract. Food Hydrocolloids 24, 770-775.

– Srinivasa, P., Ramesh, M., Kumar, K., Tharanathan, R., 2003. Properties and sorption studies of chitosan–polyvinyl alcohol blend films. Carbohydrate Polymers 53, 431-438.

– Steel, R.G., JH Dickey, D., 1997. Principles and procedures of statistics a biometrical approach. WCB/McGraw-Hill.

– Sun, Y., Yang, L., Lu, X., He, C., 2015. Biodegradable and renewable poly (lactide)–lignin composites: synthesis, interface and toughening mechanism. Journal of Materials Chemistry A 3, 3699-3709.

– Thakur, V.K., Thakur, M.K., Raghavan, P., Kessler, M.R., 2014. Progress in green polymer composites from lignin for multifunctional applications: a review. ACS Sustainable Chemistry & Engineering 2, 1072-1092.

– Toth, I.K., Bell, K.S., Holeva, M.C., Birch, P.R., 2003. Soft rot erwiniae: from genes to genomes. Molecular plant pathology 4, 17-30.

– Vicentini, D.S., Smania, A., Laranjeira, M.C., 2010. Chitosan/poly (vinyl alcohol) films containing ZnO nanoparticles and plasticizers. Materials Science and Engineering: C 30, 503-508.

– Vieira, M.G.A., da Silva, M.A., dos Santos, L.O., Beppu, M.M., 2011. Natural-based plasticizers and biopolymer films: A review. European Polymer Journal 47, 254-263.

– Voronova, M.I., Surov, O.V., Guseinov, S.S., Barannikov, V.P., Zakharov, A.G., 2015. Thermal stability of polyvinyl alcohol/nanocrystalline cellulose composites. Carbohydrate polymers 130, 440-447.

– Waleron, M., Waleron, K., Lojkowska, E., 2014. Characterization of Pectobacterium carotovorum subsp. odoriferum causing soft rot of stored vegetables. European Journal of

692 Plant Pathology 139, 457-469.
693 – Wang, K., Bauer, S., Sun, R.-c., 2012. Structural Transformation of Miscanthus ×
694 giganteus Lignin Fractionated under Mild Formosolv, Basic Organosolv, and Cellulolytic
695 Enzyme Conditions. Journal of Agricultural and Food Chemistry 60, 144-152.
696 – Xie, W., Xu, P., Liu, Q., 2001. Antioxidant activity of water-soluble chitosan derivatives.
697 Bioorganic & Medicinal Chemistry Letters 11, 1699-1701.
698 – Xu, G., Ren, S., Wang, D., Sun, L., Fang, G., 2013. Fabrication and properties of alkaline
699 lignin/poly (vinyl alcohol) blend membranes. BioResources 8, 2510-2520.
700 – Yang, W., Dominici, F., Fortunati, E., Kenny, J.M., Puglia, D., 2015a. Effect of lignin
701 nanoparticles and masterbatch procedures on the final properties of glycidyl
702 methacrylate-g-poly (lactic acid) films before and after accelerated UV weathering.
703 Industrial Crops and Products 77, 833-844.
704 – Yang, W., Fortunati, E., Dominici, F., Giovanale, G., Mazzaglia, A., Balestra, G., Kenny,
705 J., Puglia, D., 2016. Synergic effect of cellulose and lignin nanostructures in PLA based
706 systems for food antibacterial packaging. European Polymer Journal 79, 1-12.
707 – Yang, W., Fortunati, E., Dominici, F., Kenny, J., Puglia, D., 2015b. Effect of processing
708 conditions and lignin content on thermal, mechanical and degradative behavior of lignin
709 nanoparticles/polylactic (acid) bionanocomposites prepared by melt extrusion and solvent
710 casting. European Polymer Journal 71, 126-139.
711 – Yang, W., Kenny, J.M., Puglia, D., 2015c. Structure and properties of biodegradable
712 wheat gluten bionanocomposites containing lignin nanoparticles. Industrial Crops and
713 Products 74, 348-356.
714 – Ye, D.-z., Jiang, L., Hu, X.-q., Zhang, M.-h., Zhang, X., 2016. Lignosulfonate as
715 reinforcement in polyvinyl alcohol film: Mechanical properties and interaction analysis.
716 International journal of biological macromolecules 83, 209-215.
717 – Yen, M.-T., Yang, J.-H., Mau, J.-L., 2008. Antioxidant properties of chitosan from crab
718 shells. Carbohydrate Polymers 74, 840-844.
719

Table 1: Binary and ternary nanocomposite formulations

Formulations	PVA (wt %)	CH (wt %)	LNP (wt %)
PVA	100	-	-
PVA/1LNP	99	-	1
PVA/3LNP	97	-	3
CH	-	100	-
CH/1LNP	-	99	1
CH/3LNP	-	97	3
PVA/CH	90	10	-
PVA/CH/1LNP	89	10	1
PVA/CH/3LNP	87	10	3

Table 2

Table 2: Thermal parameters derived from DSC analysis of PVA, CH and PVA/CH/LNP nanocomposites

	First heating scan	*Cooling*			*Second heating scan*	
Materials	T_g *(°C)*	T_g *(°C)*	T_c *(°C)*	ΔH_c *(J/g)*	T_m *(°C)*	X_c *(%)*
PVA	84.6±0.5	-	177.6±1.2	15.8±2.6	213.2±1.2	9.8±1.6
PVA/1LNP	86.2±2.1	-	192.0±1.2	22.8±1.4	221.4±5.6	14.2±0.9
PVA/3LNP	86.9±3.1	-	201.0±0.1	28.3±1.2	225.4±0.3	18.1±0.8
CH	-	131.2±0.4	-	-	-	-
CH/1LNP	-	130.0±0.5	-	-	-	-
CH/3LNP	-	123.3±0.1	-	-	-	-
PVA/CH	90.0±2.7	-	175.8±1.2	15.7±1.3	212.8±0.5	10.8±0.9
PVA/CH/1LNP	89.3±1.5	-	184.3±0.5	25.6±0.7	218.4±0.2	17.8±0.5
PVA/CH/3LNP	89.0±2.4	-	186.1±2.9	27.6±3.4	219.4±2.0	19.6±2.4

Table 3: TGA results of PVA, CH and PVA/CH/LNP nanocomposites

Materials	Temperature at peak (°C)		Residue @ 600°C (%)
	Peak 1	Peak 2	
PVA	85.0	258.0	11.4
PVA/1LNP	94.6	266.0	11.3
PVA/3LNP	95.3	278.6	12.4
CH	59.2	280.4	28.2
CH/1LNP	77.4	276.0	32.0
CH/3LNP	79.4	278.3	36.1
PVA/CH	82.3	249.1	15.6
PVA/CH/1LNP	93.0	267.3	12.3
PVA/CH/3LNP	98.4	277.8	15.1

Table 4: Optical properties and antioxidation activity of the migrating substances for PVA, CH and PVA/CH/LNP nanocomposites

	Optical property		Antioxidation activity	
Samples	Transmittance @ 320 nm (%)	Transmittance @ 550 nm (%)	Absorption @ λ=517nm (%)	RSA (%)
PVA (Control)	90.79	94.04	0.4724	0
PVA/1LNP	24.43	78.01	0.103	78.2
PVA/3LNP	0.39	38.40	0.0522	89.0
CH	70.62	92.20	0.3765	20.3
CH/1LNP	1.83	66.70	0.1392	70.5
CH/3LNP	1.52	44.02	0.038	92.0
PVA/CH	87.73	92.71	0.3576	24.3
PVA/CH/1LNP	1.74	74.38	0.068	85.6
PVA/CH/3LNP	0.87	52.39	0.039	91.7

Table 5

Table 5: Results of color test for PVA, CH and PVA/CH/LNP nanocomposites

	PVA(control)	**PVA /1LNP**	**PVA/3LNP**	**CH**	**CH/1LNP**	**CH/3LNP**	**PVA/CH**	**PVA/CH/1LNP**	**PVA/CH/3LNP**
L*	92.03	67.44	64.92	92.36	84.18	72.47	93.33	69.17	60.05
a*	3.36	7.27	8.64	3.47	1.21	3.77	3.2	6.34	11.78
B*	13.71	60.33	61.98	14.06	34.44	56.18	13.43	60.74	68.38
ΔE	--	52.85	55.62	1.26	52.38	63.89	0.49	22.27	46.62

Figure 1

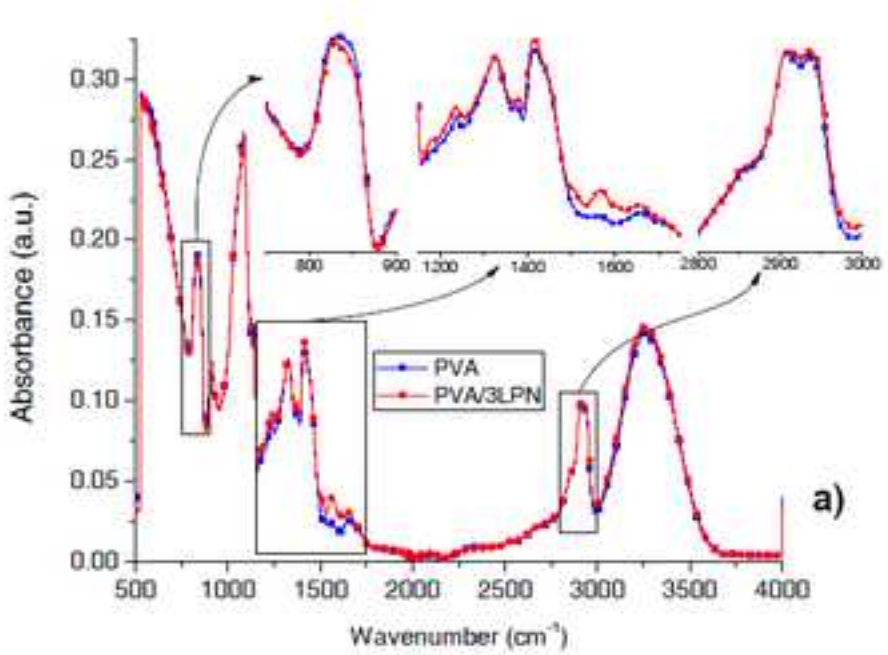
Absorbance (a.u.)
Wavenumber (cm-1)
PVA
PVA/3LPN
a)

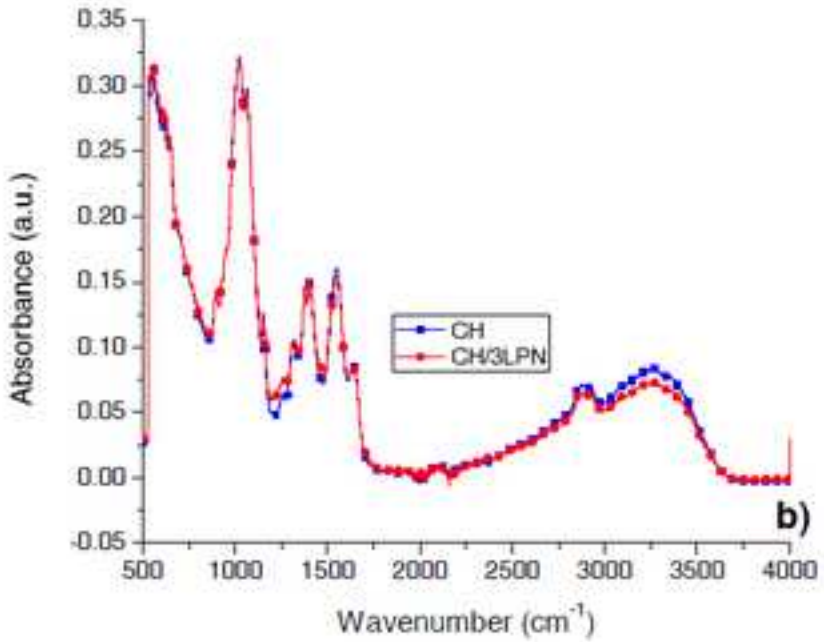
Absorbance (a.u.)
Wavenumber (cm-1)
CH
CH/3LPN
b)

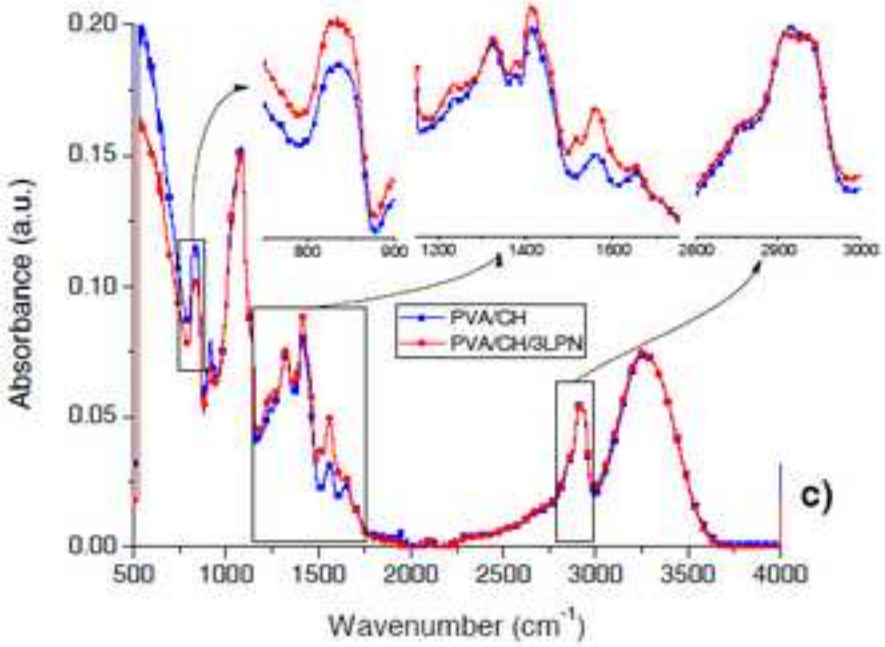
Absorbance (a.u.)
Wavenumber (cm-1)
PVA/CH
PVA/CH/3LPN
c)

Figure 2

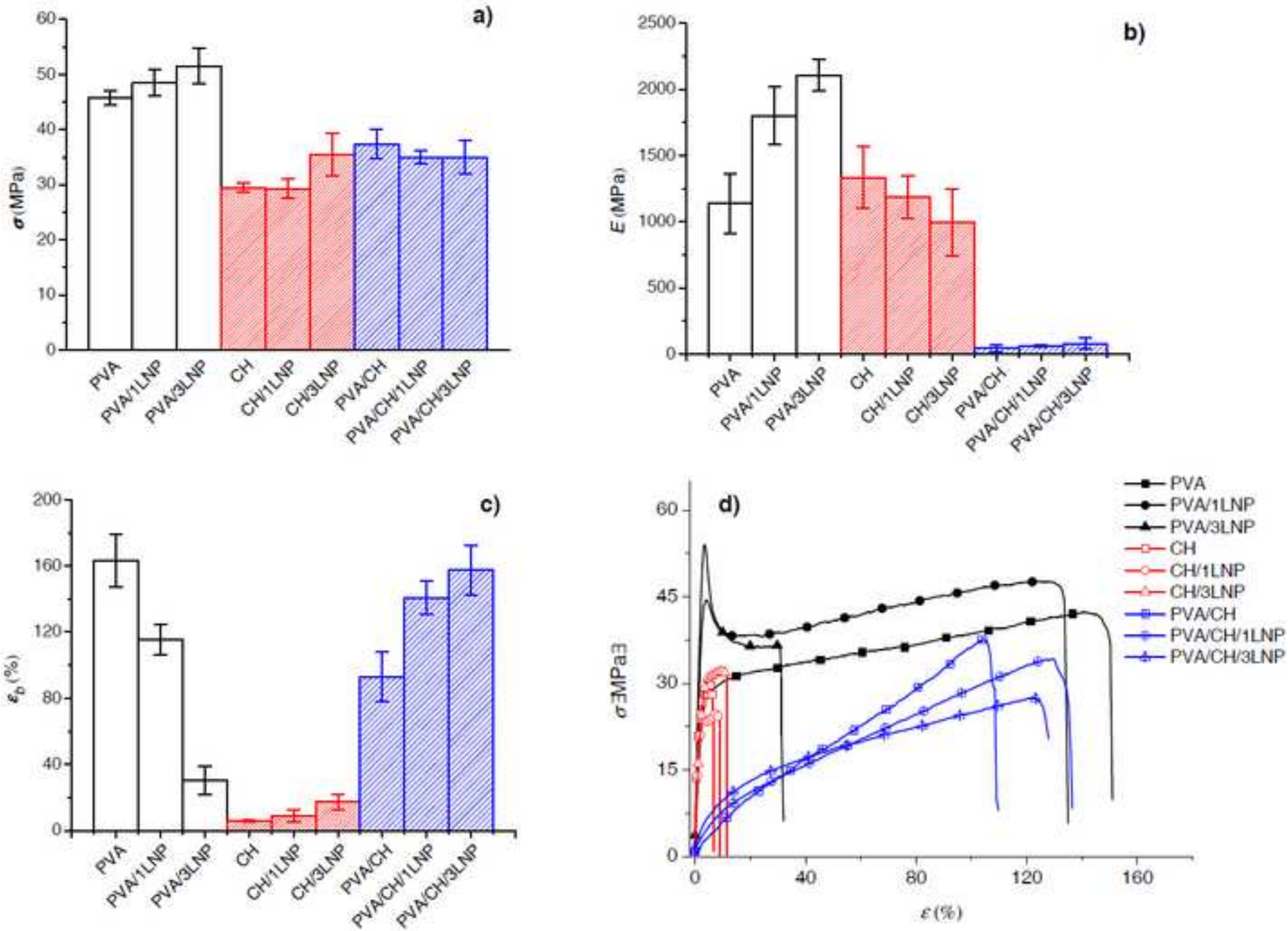
a)
σ (MPa)
0
10
20
30
40
50
60
PVA
PVA/1LNP
PVA/3LNP
CH
CH/1LNP
CH/3LNP
PVA/CH
PVA/CH/1LNP
PVA/CH/3LNP
b)
E (MPa)
0
500
1000
1500
2000
2500
c)
ε_b (%)
0
40
80
120
160
200
d)
σ/MPa
ε (%)
0
15
30
45
60
0
40
80
120
160
PVA
PVA/1LNP
PVA/3LNP
CH
CH/1LNP
CH/3LNP
PVA/CH
PVA/CH/1LNP
PVA/CH/3LNP

Figure 3

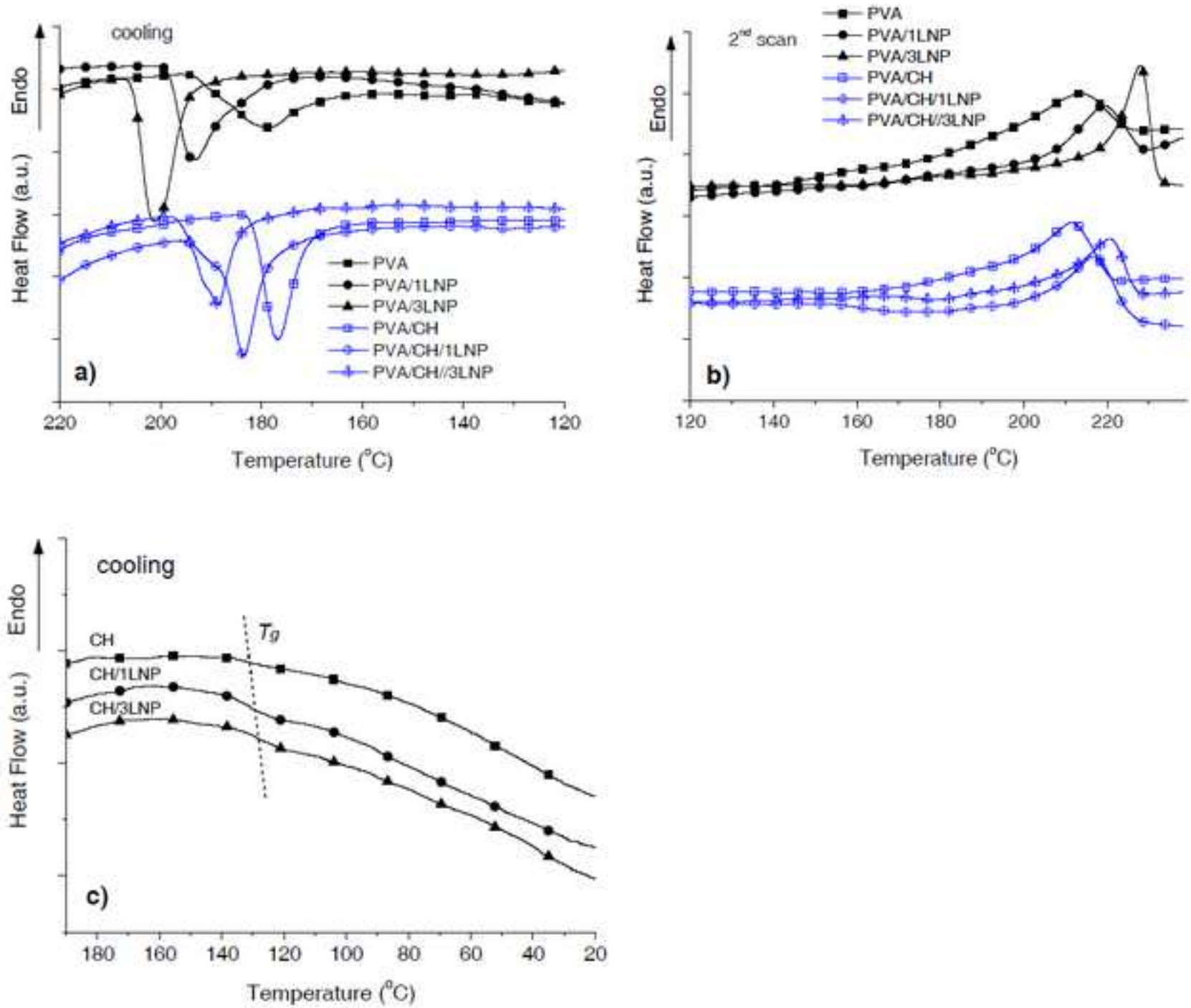
cooling
Endo
Heat Flow (a.u.)
PVA
PVA/1LNP
PVA/3LNP
PVA/CH
PVA/CH/1LNP
PVA/CH//3LNP
a)
220
200
180
160
140
120
Temperature (°C)
2nd scan
b)
CH
CH/1LNP
CH/3LNP
Tg
c)
180
160
140
120
100
80
60
40
20

Figure 4

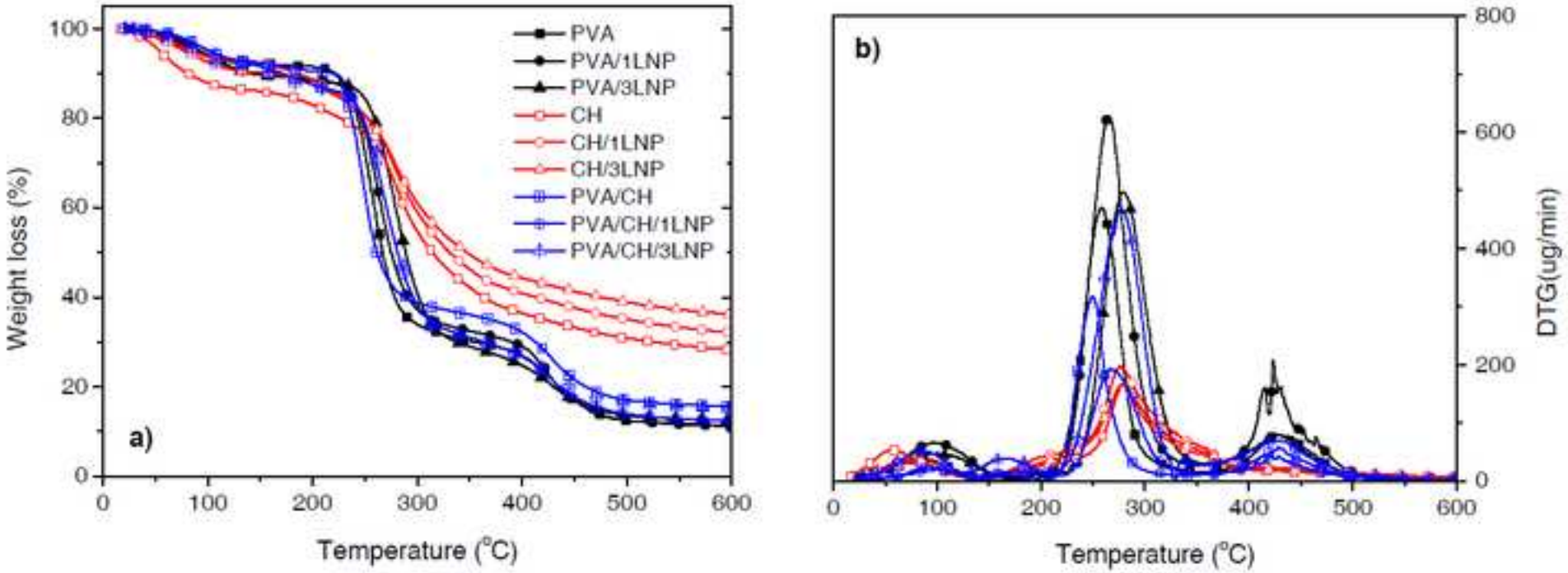
a)
Weight loss (%)
Temperature (°C)
PVA
PVA/1LNP
PVA/3LNP
CH
CH/1LNP
CH/3LNP
PVA/CH
PVA/CH/1LNP
PVA/CH/3LNP
b)
DTG(ug/min)
Temperature (°C)

Figure 5

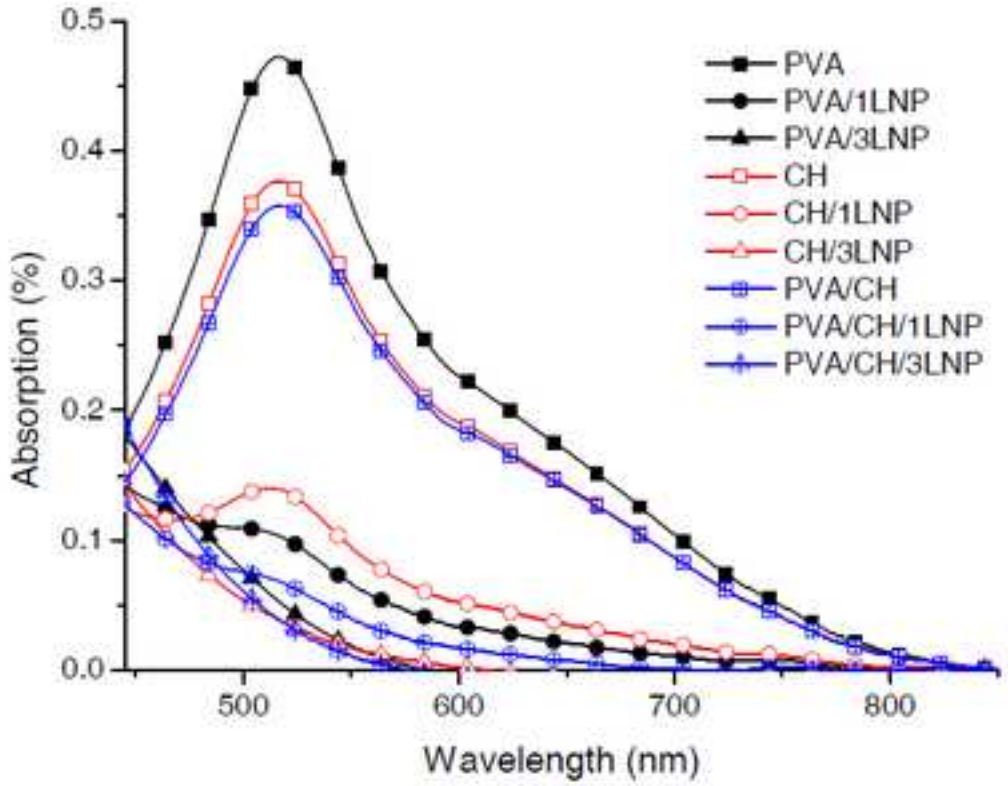
0.5
0.4
0.3
0.2
0.1
0.0
Absorption (%)
500
600
700
800
Wavelength (nm)
PVA
PVA/1LNP
PVA/3LNP
CH
CH/1LNP
CH/3LNP
PVA/CH
PVA/CH/1LNP
PVA/CH/3LNP

a)

b)

Figure 6

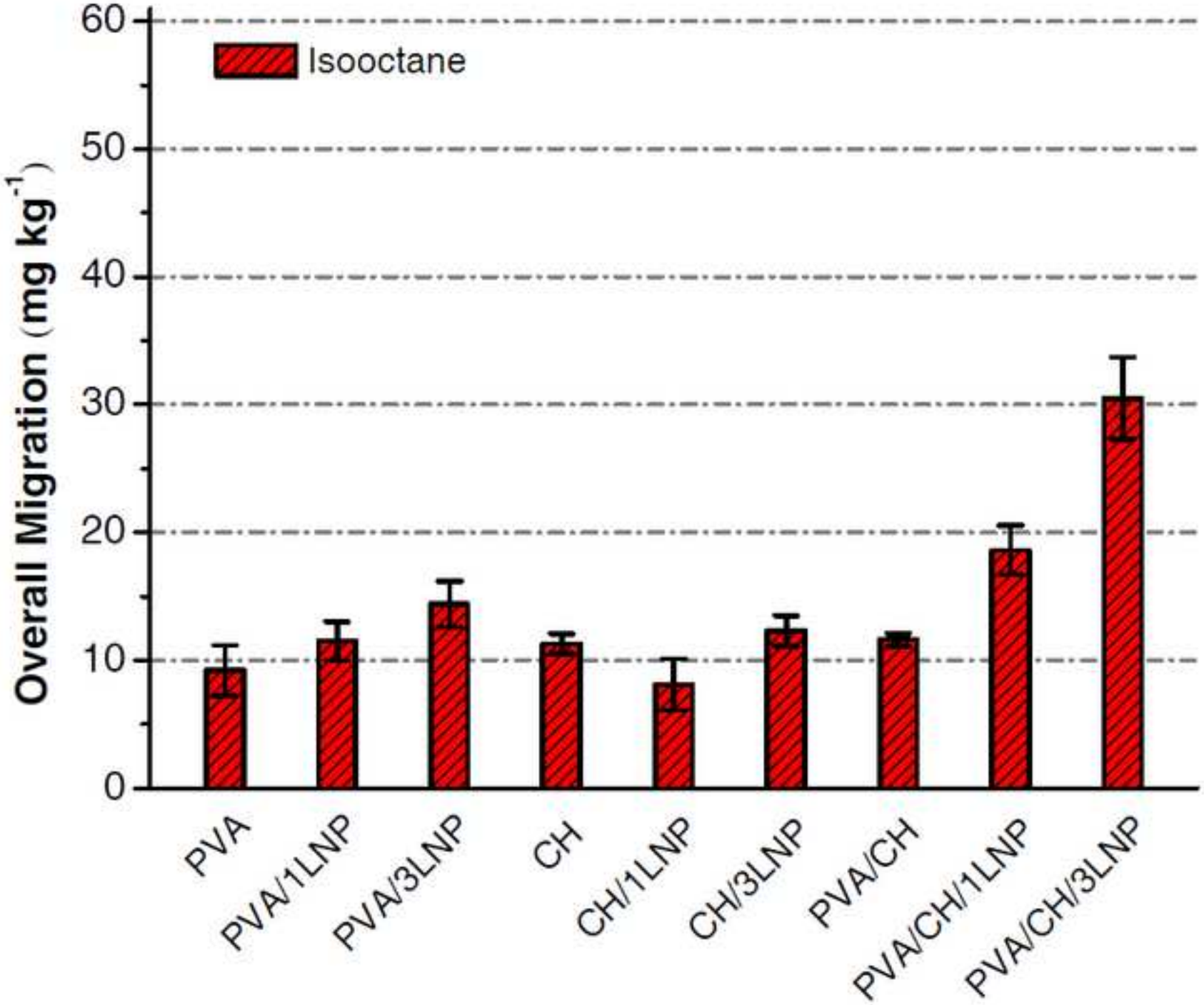
Isooctane
Overall Migration (mg kg-1)
60
50
40
30
20
10
0
PVA
PVA/1LNP
PVA/3LNP
CH
CH/1LNP
CH/3LNP
PVA/CH
PVA/CH/1LNP
PVA/CH/3LNP

Figure 7

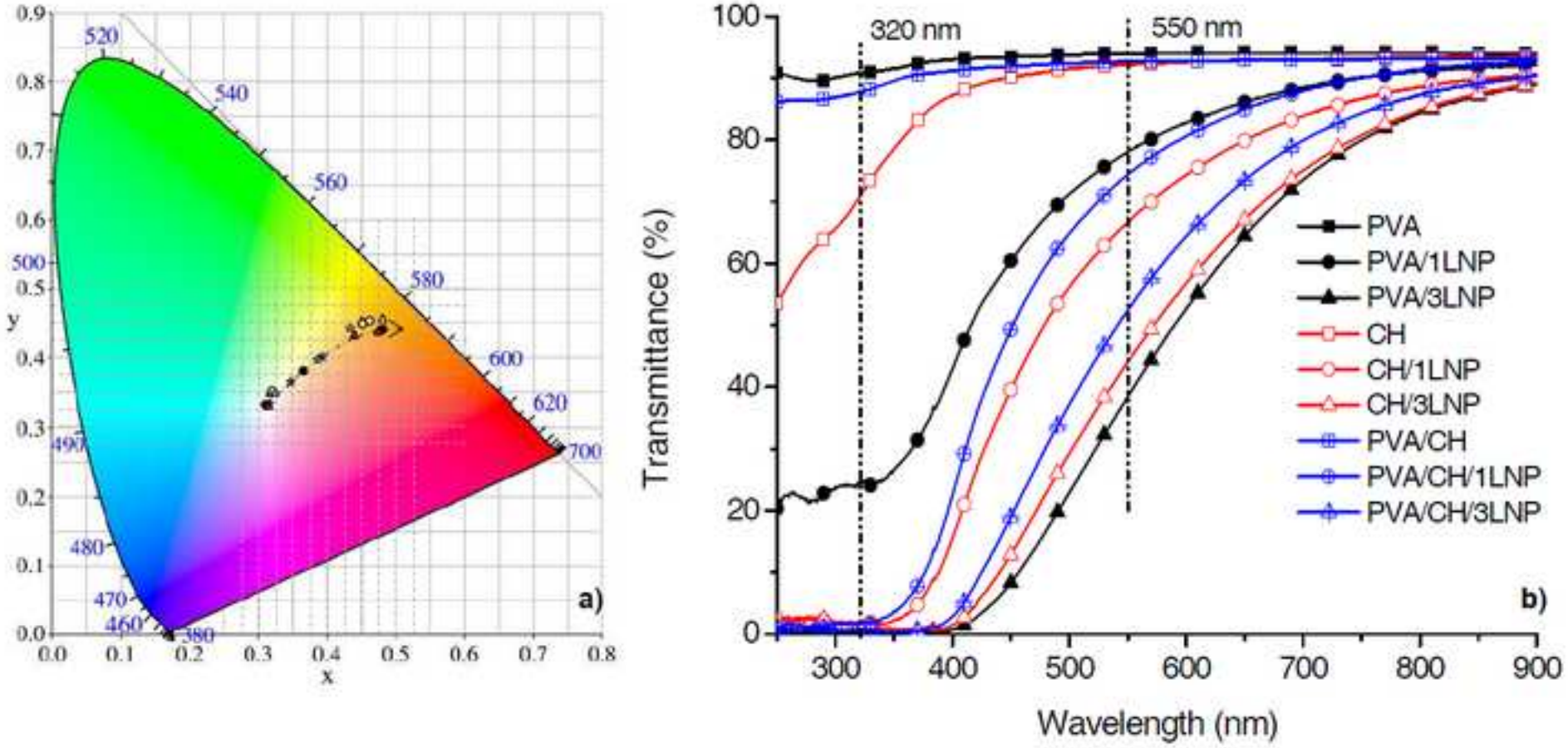
a)
x
y
520
540
560
580
600
620
700
500
490
480
470
460
380
b)
320 nm
550 nm
Transmittance (%)
Wavelength (nm)
PVA
PVA/1LNP
PVA/3LNP
CH
CH/1LNP
CH/3LNP
PVA/CH
PVA/CH/1LNP
PVA/CH/3LNP

Figure 8

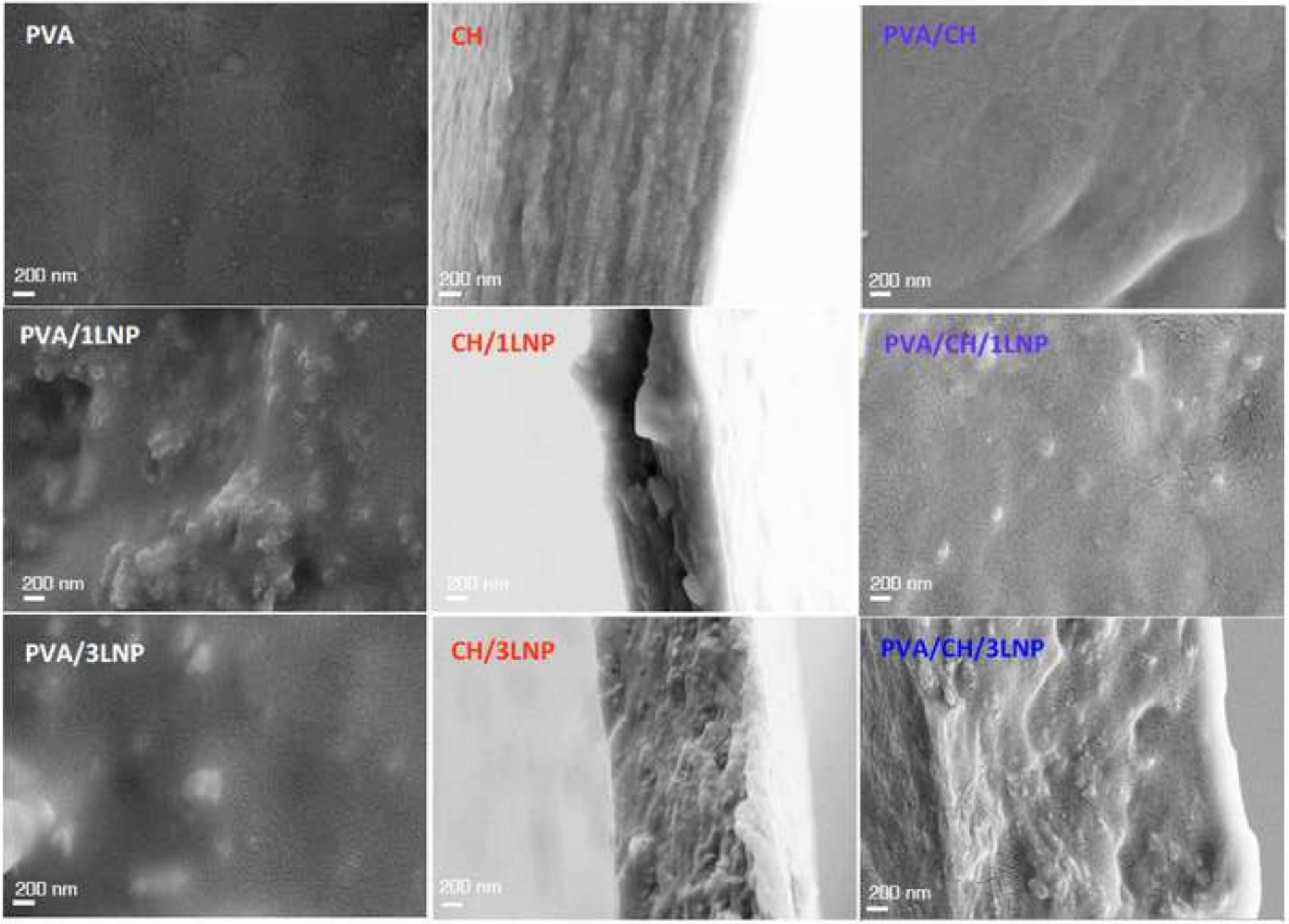
PVA
200 nm
CH
200 nm
PVA/CH
200 nm
PVA/1LNP
200 nm
CH/1LNP
200 nm
PVA/CH/1LNP
200 nm
PVA/3LNP
200 nm
CH/3LNP
200 nm
PVA/CH/3LNP
200 nm

Figure 9a

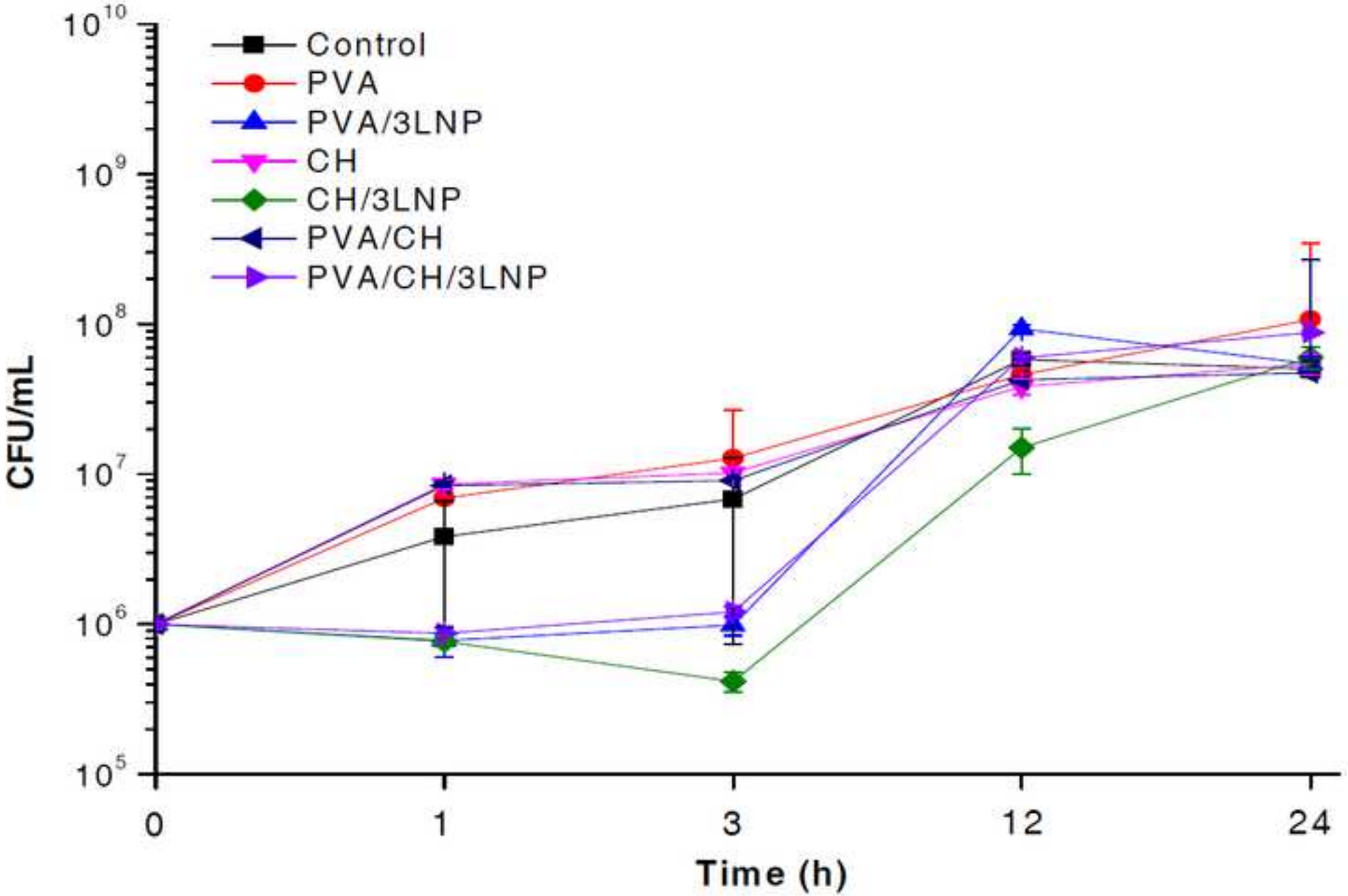
Control
PVA
PVA/3LNP
CH
CH/3LNP
PVA/CH
PVA/CH/3LNP
CFU/mL
10^{10}
10^{9}
10^{8}
10^{7}
10^{6}
10^{5}
0
1
3
12
24
Time (h)

Figure 9b

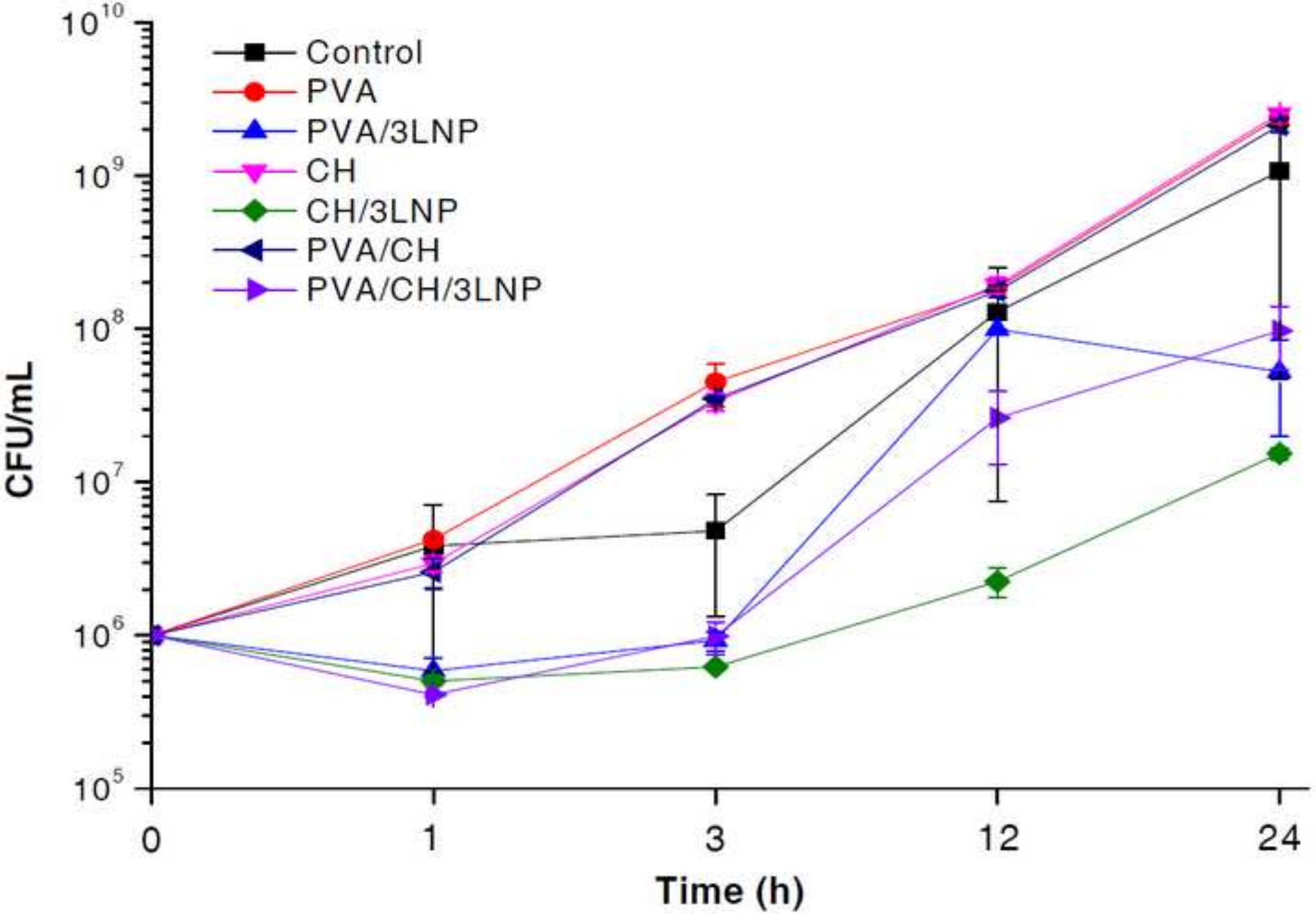
Control
PVA
PVA/3LNP
CH
CH/3LNP
PVA/CH
PVA/CH/3LNP
CFU/mL
10^{10}
10^{9}
10^{8}
10^{7}
10^{6}
10^{5}
0
1
3
12
24
Time (h)